Low-Temperature Electrical and Thermal Resistivities of Tungsten†

D. K. Wagner
Laboratory of Atomic and Solid State Physics, Cornell University, Ithaca, New York 14850

and

J. C. Garland
Department of Physics, The Ohio State University, Columbus, Ohio 43210

and

R. Bowers
Laboratory of Atomic and Solid State Physics, Cornell University, Ithaca, New York 14850

(Received 13 January 1971)

Measurements of ρ and WT (ρ is the electrical resistivity and W is the thermal resistivity) of high-purity single-crystal specimens of tungsten have been performed in the temperature range 1.5–6.0 K. The temperature dependence of ρ and WT was found to be predominantly quadratic, in agreement with observations in other transition metals. We attribute this behavior to electron-electron scattering between different branches of the Fermi surface. The validity of Matthiessen's rule for impurity and boundary scattering was investigated to determine whether the contributions of electron-electron scattering ρ_e and W_eT could be meaningfully separated from the total resistivities ρ and WT. In those samples in which boundary scattering contributed least to the total resistivities, Matthiessen's rule was found to be reasonably well obeyed for the electrical resistivity, while deviations were observed for the thermal resistivity. The Lorenz number for electron-electron scattering, $L_e=\rho_e/W_eT$, for these samples was found to range from 0.2×10^{-8} to 0.4×10^{-8} W Ω/K².

I. INTRODUCTION

Recently, the low-temperature electrical and thermal resistivities of several transition metals (Ni, Re, Pd, Os, Pt, and Fe)[1–7] have been measured. These studies have been important in revealing a T^2 behavior of both the electrical resistivity ρ and the analogous thermal transport property WT (W is the thermal resistivity) at low temperatures. The T^2 behavior of the electrical resistivity ρ of a number of transition metals has been known for many years[8] and was first attributed to electron-electron scattering between different branches of the Fermi surface.[9] Since that time, the observation of the T^2 behavior of WT at low temperatures in Ni, Re, Pd, Pt, and Fe has lent further support to the view that electron-electron scattering can be an important resistive mechanism in many transition metals.[10,11]

This paper describes the extension of these measurements to tungsten. We have made a detailed study of the temperature dependence of ρ and WT in a number of high-purity tungsten single crystals and have observed a dominant T^2 dependence for both ρ and WT in the temperature range 1.5–6.0 K. In order to determine reliably the magnitudes of the T^2 terms in the resistivities, we have also examined the validity of Matthiessen's rule for electron-electron scattering—that is, the extent to which the coefficients of the T^2 terms in the resistivities are not affected by other scattering mechanisms such as impurity scattering and boundary scattering.

Considerable effort has been devoted to estimating theoretically the relative magnitudes of the T^2 term ρ_e in ρ and the T^2 term W_eT in WT.[12–18] Because of the difficulty of estimating the magnitudes of ρ_e and W_e separately, several calculations have been performed that give the ratio $L_e=\rho_e/W_eT$, the Lorenz number for electron-electron scattering. The first such calculation was performed by Herring[12] in connection with the measurements of ρ_e and W_eT in nickel by White and Tainsh.[1] Herring argued that the assumption of a complicated Fermi surface could result in a considerable simplification of the collision integral for electron-electron scattering, thus making it possible to obtain an energy-dependent relaxation time. In the absence of impurity scattering, this relaxation time leads to a value of L_e of 1.58×10^{-8} W Ω/K², while for situations in which impurity scattering is predominant over electron-electron scattering, a value of 1.36×10^{-8} W Ω/K² is obtained.[13] Although his argument does not assume any particular form for the scattering rate, Herring has noted that L_e can be quite sensitive to the angular distribution of the scattering. It is perhaps for this reason that agreement with experiment has not been particularly good. Measurements of the transport properties of Ni, Re, Pd, Pt, and Fe have yielded various values of L_e: 1.0 for Ni,[1] 0.9 for Re,[2,4] 1.1 for Pd,[3,4] 0.1 for

Pt, [6] and 1.2 for Fe, [7] each in units of 10^{-8} W Ω/K^2.

Other models have been considered that allow calculation of L_e for a particular scattering rate. Initial progress in this direction was made by Smith and Wilkins, [14] who found solutions to the linearized Boltzmann equation for combined electron-electron scattering and impurity scattering on a spherical Fermi surface. While this model can be expected to appropriately describe normal electron-electron scattering[15] in simple metals, it cannot be applied to the transition metals which have considerably more complicated band structures. Bennett and Rice[16] have modified this calculation to describe the scattering of mobile "*s*" electrons in one band by heavier "*d*" holes in another. To make the calculation tractable they have assumed spherical "*s*" and "*d*" bands, and, in addition, have assumed that the current is carried primarily by the "*s*" electrons. Although this model is still an oversimplification of the band structures of the transition metals, it is, nevertheless, instructive because it exhibits certain features that would probably be retained in a more realistic model. In particular, their calculation shows that L_e depends rather sensitively on the angular distribution of the electron-electron scattering. In the limit of small-angle scattering, L_e approaches zero, while for isotropic scattering, L_e approaches a value between 1.36×10^{-8} and 1.58×10^{-8} W Ω/K^2, the exact value depending upon the amount of impurity scattering present. For intermediate angular dependences of the scattering rate, these calculations show that L_e can assume values between zero and the values calculated by Herring. Bennett and Rice point out that a scattering rate corresponding to a screened Coulomb interaction leads to values of L_e between about 0.8×10^{-8} and 1.0×10^{-8} W Ω/K^2 in a typical transition metal; this is in reasonable agreement with the experimental results for Ni, [10] Re, Pd, and Fe, but not Pt. These calculations also show that significant deviations from Matthiessen's rule can occur when impurity scattering and electron-electron scattering act together. The effect is largest in the thermal resistivity, causing about a 30% increase in $[WT-(WT)_0]$ as the amount of impurity scattering is increased. In the electrical resistivity, a smaller, approximately 10%, increase in $(\rho-\rho_0)$ occurs.

Other calculations have been carried out by Rice, [17] and Schriempf, Schindler, and Mills[18] using a spherical two-band model for the Fermi surface and a screened Coulomb interaction between electrons. Because a specific scattering rate is postulated, these treatments are special cases of the calculation of Bennett and Rice and lead to similar results.

To our knowledge, no measurements of the thermal resistivity of high-purity tungsten have been made in the liquid-helium temperature range. Measurements at higher temperatures in a restricted range (14–22 K) have been made by de Nobel, [19] who finds that WT can be described by $WT=(WT)_0+\beta T^3$ with $\beta\approx5\times10^{-5}$ cm/W K. However, this temperature range is not sufficiently large, nor the data sufficiently precise, to distinguish between a βT^3 temperature dependence (electron-phonon scattering only) and a $\alpha T^2+\beta T^3$ temperature dependence (electron-electron and electron-phonon scattering).

Studies of the temperature dependence of the electrical resistivity of high-purity tungsten have been made by Volkenshteyn *et al.* [20] and Berthel[21] over a wide range of temperatures. Volkenshteyn *et al.* have measured the electrical resistivity of a sample with a residual resistance ratio $[\rho(300\text{ K})/\rho(4.2\text{ K})]$ of 19 000 over a temperature range 4–300 K. They find that at low temperatures[22] the resistivity can be described by $\rho=\rho_0+AT^2+BT^5$ with $A=40\times10^{-13}$ Ω cm/K^2 and $B=0.8\times10^{-15}$ Ω cm/K^5. Berthel has measured the electrical resistivity of a number of single-crystal tungsten rods with residual resistance ratios $[\rho(273\text{ K})/\rho(0\text{ K})]$ ranging over 15 000–330 000. His measurements were made in two temperature ranges: 1.4–4.2 K and 14–27 K. In the 1.4–4.2-K range, he finds that $\rho=\rho_0+AT^2$ with $A=8\times10^{-13}$ Ω cm/K^2 in the samples in which boundary scattering contributes least to the resistivity. In the samples in which boundary scattering contributes significantly to the resistivity, the coefficient A is enhanced. In the 14–27-K temperature range, he finds that $\rho=\rho_0+C+BT^5$ with $B=0.6\times10^{-15}$ Ω cm/K^5. Thus there is reasonable agreement between measurements on the magnitude of the T^5 term, but a considerable lack of agreement on the size of the T^2 term.

Berthel[21] has pointed out that in less-pure samples $[\rho(273\text{ K})/\rho(0\text{ K})\leq1500]$ investigated earlier by other workers, [23,24] the temperature dependence of ρ is considerably different from that of the pure samples; in fact, the electrical resistivity does not appear to exhibit a T^5 behavior at any temperature. Qualitatively, the magnitude of the temperature-dependent part of the resistivity increases and the dependence on temperature weakens as the impurity content of the sample is increased. For example, in a polycrystalline tungsten sample with a residual resistance ratio $[\rho(295\text{ K})/\rho(0\text{ K})]$ of 180, White and Woods[24] observed a T^4 temperature dependence above 20 K and a T^2 dependence at lower temperatures. They measure a coefficient A of the T^2 term of 100×10^{-13} Ω cm/K^2, more than ten times larger than the coefficient measured by Berthel in high-purity single-crystal samples. The wide variation with purity

of the temperature dependence of the electrical resistivity emphasizes the need to study deviations from Matthiessen's rule in experimental studies of transport processes in tungsten.

Size-effect studies in tungsten have been carried out by Berthel[25] and by Startsev *et al.*[26] in order to determine the electronic mean free path. Startsev *et al.* have performed careful measurements on tungsten single crystals of square cross section. They reduced the thickness in small increments by more than a factor of 20 by electroetching, and were especially careful to eliminate errors due to an inhomogenous distribution of impurities in the samples. Although they attempted to estimate a bulk mean free path λ_B from their measurements by assuming a very simple model for the size effect, values of λ_B obtained in this way were not independent of sample diameter. Without a more sophisticated treatment of the dc size effect than is presently available, there is no reliable way to determine λ_B from the measured resistivity and specimen size. Roughly speaking, however, Startsev *et al.* estimated that boundary scattering contributed about 60% to the resistivity of a specimen whose thickness was 1.5 mm and whose residual resistance ratio was 30 000.

II. EXPERIMENTAL DETAILS

The cryostat shown in Fig. 1 was designed so that the electrical and thermal resistivities could be measured during the same experiment.

The thermal resistivity W was determined by the usual method of measuring the temperature difference ΔT produced between two points on the sample by a known heat current $\dot{Q}$. However, rather than computing the temperature difference directly from the measured temperatures at the two points on the sample, as is customarily done, we have used a differential technique that makes a direct comparison of the temperature along the sample with the heat current on and with it off. This technique is particularly suited to the use of small temperature differences (< 30 mK), and since it is not commonly used for this type of measurement, we give a brief explanation of the method.

One end of the tungsten sample was electroplated with copper and soldered securely to a copper platform whose temperature could be regulated electronically by means of a heater H_2 and a carbon sensing thermometer R_3. Another heater H_1, used to generate the heat current Q through the sample, was attached to the other end. In order to measure the resulting temperature difference ΔT across the sample, two carbon resistance thermometers[27] R_1 and R_2 were soldered to copper rings electroplated to the tungsten sample about 12 cm apart. These two thermometers were connected in two arms of a Wheatstone bridge in such a way that R_1 and $\Delta R \equiv R_1 - R_2$ could be measured directly. The bridge was operated at 85 Hz, and the null in the output was detected with a phase-lock amplifier. During each experiment, R_1 and ΔR were calibrated against a standard germanium resistance thermometer[28] R_4 attached to the copper platform. The resistance of this thermometer was measured by means of a specially designed four-terminal bridge described elsewhere,[29] allowing measurement of the absolute temperature to an accuracy of at least 5 mK. All of the electrical leads from the sample were thermally anchored to the copper platform.

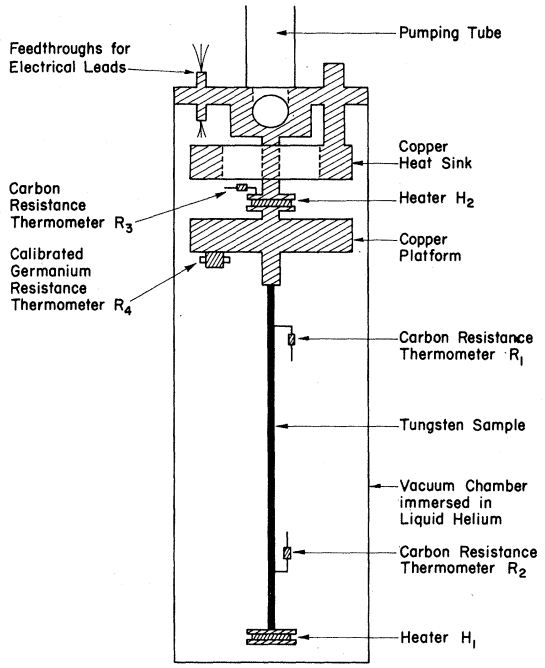

FIG. 1. Diagram of the cryostat. Electrical leads are brought into the vacuum chamber via Epoxy feedthroughs and are anchored thermally to the heat sink. From the heat sink, short constantan wires run to the copper platform where they are again thermally anchored. From the platform, connections are made to the sample.

The thermal resistivity was measured as follows: First, $\Delta R(T, \Delta T) \equiv R_1(T) - R_2(T + \Delta T)$ and $R_1(T)$ were measured with a heat current $\dot{Q}$ flowing in the sample. Next, the heat current was reduced to zero and the temperature of the platform was adjusted by means of the regulator to keep R_1 at the same temperature, and then $\Delta R(T, 0) = R_1(T) - R_2(T)$ was measured. The temperature difference ΔT was calculated by the expression

$$\Delta T = -[\Delta R(T, \Delta T) - \Delta R(T, 0)] \Big/ \frac{dR_2}{dT} , \qquad (1)$$

which is valid provided $(dR_2/dT) \gg \frac{1}{2}(d^2R_2/dT^2)(\Delta T)$ (see Appendix). Finally, the thermal resistivity W was calculated from $W = (\Delta T/\dot{Q})(A/L)$, where

A/L is the ratio of the cross-sectional area A of the specimen and the distance L between the copper rings. This ratio was determined by measuring the resistance of the sample at room temperature, using a value of 5.38 $\mu\Omega$ cm for the room-temperature resistivity to compute A/L; in computing this ratio we have neglected the small change that occurs because of contraction as the sample is cooled to liquid-helium temperature. We verified that the thermal resistivity W was independent of the heat current used for a tenfold change in heat current and were able to calculate W to a precision of about 1% for the samples with diameters of 1.5 mm or smaller, and to a precision of about 8% for the 3.0-mm samples. The peak in the thermal conductivity of each of the samples occurred at about 4 K, and in the purest specimen the peak value was 750 W/cm K (the room-temperature thermal conductivity of tungsten is 1.3 W/cm K). The samples, their diameters, and other pertinent characteristics are listed in Table I.

The electrical resistivity was measured in the customary four-probe manner. Two fine-copper voltage leads were attached to the sample at the points where the thermometers were attached, and a superconducting wire was used as the current lead. A constant current was passed through the sample, and the potential produced between the voltage leads was measured by a Keithley 148 nanovoltmeter with an integrating digital voltmeter readout. We used a current of 2 A in the 1.0- and 1.5-mm-diam samples and 4 A in the 3.0-mm-diam samples. By making measurements at different currents, we verified that there were no measurable deviations from Ohm's law at these current levels due to the large magnetoresistance of tungsten. In these samples, we were able to measure the resistivity ρ to a relative precision of about $\frac{1}{2}$%. An exception occurred in the sample with the smallest diameter (sample W-8A). In this sample, we observed a resistance that decreased slightly with measuring current. We therefore used a current of 1 A to minimize this effect, thereby incurring an error of at most 2%.

Considerable care was taken to eliminate two potential sources of systematic error in the thermal measurements: (i) loss of heat from the sample via the electrical leads, and (ii) loss of heat from the sample via conduction by residual helium gas in the vacuum chamber surrounding the sample. In the first case, the loss of heat through the constantan heater and the thermometer wires was negligible. To verify that there was no significant heat loss through the copper voltage leads and the superconducting current lead, we disconnected these wires and remeasured the thermal resistivity for two samples W-3 and W-7. In each

TABLE I. Characteristics of the tungsten samples.

Sample[a]	Surface condition	Diameter (mm)	r_R	r_R/d (mm^{-1})	ρ_0 ($10^{-10}\ \Omega$ cm)	$(WT)_0$ (10^{-2} K^2 cm/W)	A (10^{-13} Ω cm/K^2)	B (10^{-15} Ω cm/K^2)	α (10^{-4} cm/W)	$L_e = A/\alpha$ (10^{-8} WΩ/K^2)	$\rho_0/(WT)_0$ (10^{-8} WΩ/K^2)
W-2	mirror	1.5	59 000	39 000	0.912 ± 0.002	0.386 ± 0.004	6.8 ± 0.3	1.1 ± 0.1	...	...	2.36 ± 0.03
W-3	mirror	1.5	43 000	29 000	1.231 ± 0.004	0.491 ± 0.004	7.2 ± 0.5	1.6 ± 0.2	2.51 ± 0.02	0.29 ± 0.06	2.51 ± 0.02
W-4	matt	1.0	30 000	30 000	1.780 ± 0.004	0.721 ± 0.005	7.4 ± 0.4	1.5 ± 0.2	2.55 ± 0.03	0.29 ± 0.02	2.47 ± 0.02
W-5	matt	1.5	9400	6300	5.724 ± 0.006	2.266 ± 0.014	6.2 ± 0.6	1.8 ± 0.3	2.91 ± 0.08	0.21 ± 0.02	2.53 ± 0.02
W-6	mirror	3.0	63 000	21 000	0.848 ± 0.012	0.316 ± 0.010	6.7 ± 1.1	1.3 ± 0.4	2.21 ± 0.08	0.30 ± 0.05	2.68 ± 0.08
W-7	mirror	3.0	95 000	32 000	0.566 ± 0.004	0.214 ± 0.010	8.7 ± 0.3	0.8 ± 0.1	2.17 ± 0.06	0.40 ± 0.02	2.64 ± 0.11
W-8	mirror	1.5	75 000	50 000	0.695 ± 0.006	0.319 ± 0.002	11.0 ± 0.6	1.3 ± 0.3	2.53 ± 0.01	(0.44 ± 0.02)	2.18 ± 0.02
W-8A	matt	~ 0.8	31 000	~ 40 000	1.748 ± 0.006	0.717 ± 0.004	12.2 ± 0.6	0.7 ± 0.3	2.78 ± 0.02	(0.44 ± 0.02)	2.44 ± 0.01
W-8B	matt	1.5	53 000	35 000	1.006 ± 0.012	0.426 ± 0.006	9.7 ± 1.4	1.0 ± 0.6	2.48 ± 0.03	(0.39 ± 0.06)	2.36 ± 0.03

[a] All samples have a [110] axis oriented along the rod axis except W-2 which has a [111] orientation. The errors shown represent 95% confidence limits (two standard deviations) calculated from the rms deviation of the data from the fit.

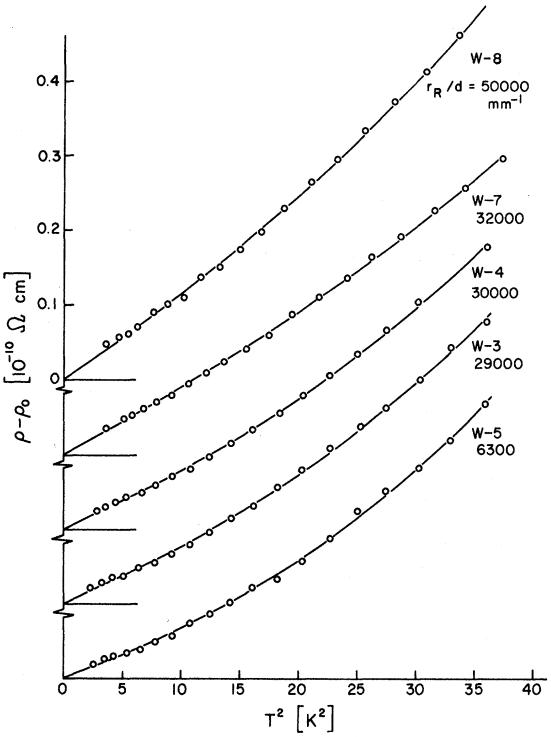

FIG. 2. Variation of the temperature-dependent part of the electrical resistivity ($\rho-\rho_0$) with T^2 for five single-crystal tungsten samples, each oriented with the [110] direction parallel to the rod axis. The origin of each plot has been displaced vertically for clarity, and the plots have been arranged in order of r_R/d. Each of the solid curves represents a function of the form AT^2+BT^5, determined by the method of least squares.

case, the measurements produced results completely consistent with the original measurements made with the wires in place. We also verified that conduction through the vacuum space was negligible by changing the temperature between the walls of the chamber and the sample; in addition, an adsorbent[30] was placed in the vacuum chamber to adsorb residual helium gas.

III. EXPERIMENTAL RESULTS

We have measured the resistivities of seven electron-beam zone-refined single-crystal tungsten specimens, six of which were oriented with the [110] direction parallel to the rod axis, and one with the [111] direction parallel to the rod axis (see Table I).

In Fig. 2, we have plotted the temperature-dependent part of the electrical resistivity ($\rho-\rho_0$) as a function of the square of the temperature for five tungsten specimens of various diameters and purities, each oriented with the [110] direction parallel to the rod axis. The most notable feature of Fig. 2 is the large temperature dependence of the resistivity for sample W-8 compared to the other samples. Similar results have been reported by Berthel,[21] who shows convincingly that this is due to the size effect. As a measure of the relative importance of boundary scattering, we have used the parameter r_R/d to characterize our samples [where r_R stands for the residual resistance ratio $\rho(299\text{ K})/\rho(0\text{ K})$ of a specimen with diameter d]. Except in the extreme size-effect regime (where r_R/d tends to a constant value), we expect r_R/d to increase roughly with increasing boundary scattering. As expected, sample W-8 has the largest value of r_R/d, although sample W-7—which does not show an enhancement of the temperature-dependent resistivity—has the largest residual resistance ratio.

The temperature dependence of the electrical resistivity of all of the samples can be adequately described by $\rho=\rho_0+AT^2+BT^5$ for the temperature range covered in this experiment. For those samples in which Matthiessen's rule is approximately obeyed, it is reasonable to identify each of these terms with the unique contributions of impurity and boundary, electron-electron, and

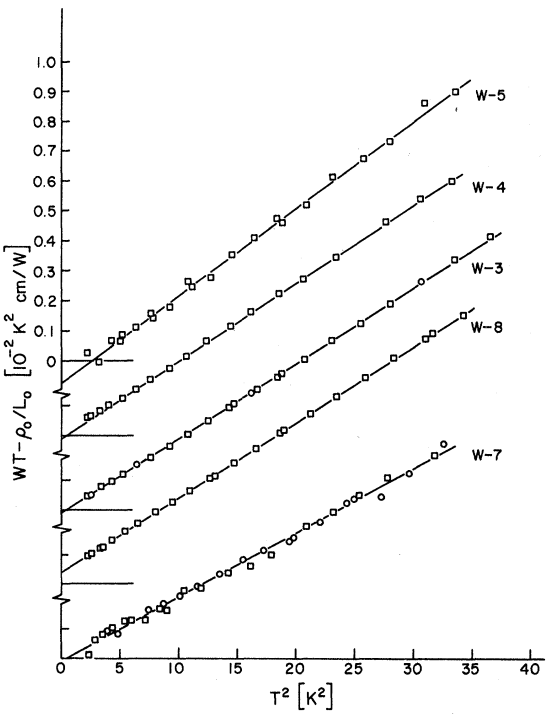

FIG. 3. Variation of $WT-\rho_0/L_0$ with T^2 for five single-crystal tungsten samples, each oriented with the [110] direction parallel to the rod axis. Origin of each plot has been displaced vertically for clarity, and the plots have been arranged in order of r_R. Square data points were taken with the potential leads and current lead attached to the sample, while the circled points were taken in a separate experiment with these leads disconnected.

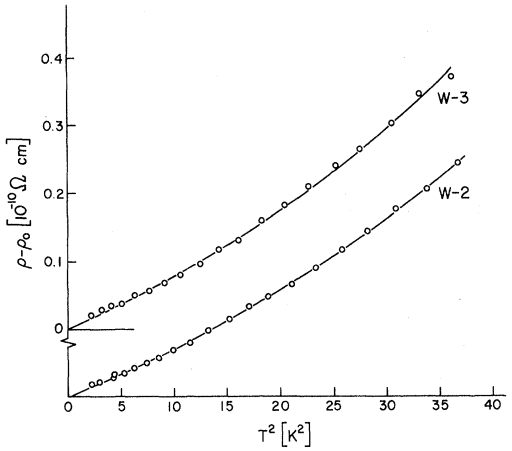

FIG. 4. Comparison of the temperature-dependent part of the electrical resistivity ($\rho-\rho_0$) for two single-crystal tungsten samples with different crystalline orientations. Samples W-2 and W-3 were oriented with the [111] and [110] directions parallel to the rod axis, respectively.

electron-phonon scattering. Although the real situation may be more complicated, there does not exist at present a more soundly based expression having as few parameters; consequently, we have been obliged to use this expression to fit our data. The values of ρ_0, A, and B were determined by the method of least squares for each of the samples and are tabulated in Table I.

In Fig. 3, we show the variation of WT with T^2 for each of the five tungsten samples shown in Fig. 2. The temperature dependence of WT can be described by $WT=(WT)_0+\alpha T^2$. A βT^3 term in WT, corresponding to the BT^5 term in ρ due to electron-phonon scattering, is not evident in the data; if such a term is present, the coefficient β would have to be smaller than 5×10^{-6} cm/WK. As shown in Table I, the value of α varies by about 30% among the samples oriented with the [110] direction along the rod axis. In general, the value of α tends to increase with increasing impurity content, although sample W-8 appears again to be an exception.

These measurements were performed mainly on specimens with the [110] direction parallel to the rod axis; however, one specimen W-2 with the [111] direction parallel to the rod axis was also studied. In Figs. 4 and 5, we compare the resistivities of samples W-2 and W-3. Although the temperature dependence of the electrical resistivities for the two samples are nearly identical, the temperature dependence of the thermal resistivities are qualitatively different; sample W-3 appears to exhibit a quadratic temperature variation, whereas sample W-2 increases at a somewhat faster rate. Ordinarily, in bulk material the resistivities of a cubic crystal, such as tungsten, must be isotropic because of the symmetry of the lattice. However, in specimens with significant amounts of boundary scattering, exceptions can be expected to occur.[31]

In Fig. 6, we show the variation of the Wiedemann-Franz ratio ρ/WT with temperature for the six samples plotted in Figs. 2–5. The Wiedemann-Franz ratios of the samples in which boundary scattering is not appreciable (W-3, W-4, W-5, and W-7) extrapolate to within a few percent of the Lorenz number $L_0=2.44\times10^{-8}$ W Ω/K^2 as the temperature approaches absolute zero. This behavior is expected when the scattering is dominated by elastic impurity scattering.[32] On the other hand, sample W-8, for which boundary scattering is expected to be appreciable, shows a departure from the Wiedemann-Franz law that is many times larger than the limits set by the random error in the experiment.

We performed further measurements on sample W-8 in an attempt to clarify this effect. Sample W-8 was spark cut into two shorter rods of equal length. The residual resistance ratio of each half was measured and was found to be essentially the same as that of the original sample. One side of one of the pieces was removed by electroetching to produce a specimen with a smaller effective diameter (semicircular cross section) but with substantially the same mean impurity content. This sample was designated W-8A. The other piece was electroetched uniformly for a short period to remove the mirror finish of sample W-8, resulting in a sample with a matt finish identical to that of W-8A, but with a diameter essentially

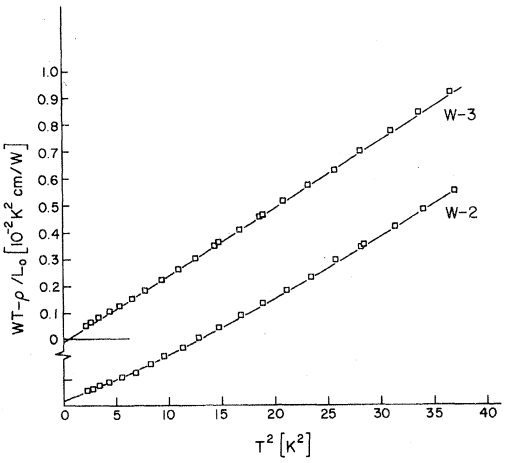

FIG. 5. Comparison of ($WT-\rho_0/L_0$) for two single-crystal tungsten samples with different crystalline orientations. Samples W-2 and W-3 were oriented with the [111] and [110] directions parallel to the rod axis, respectively.

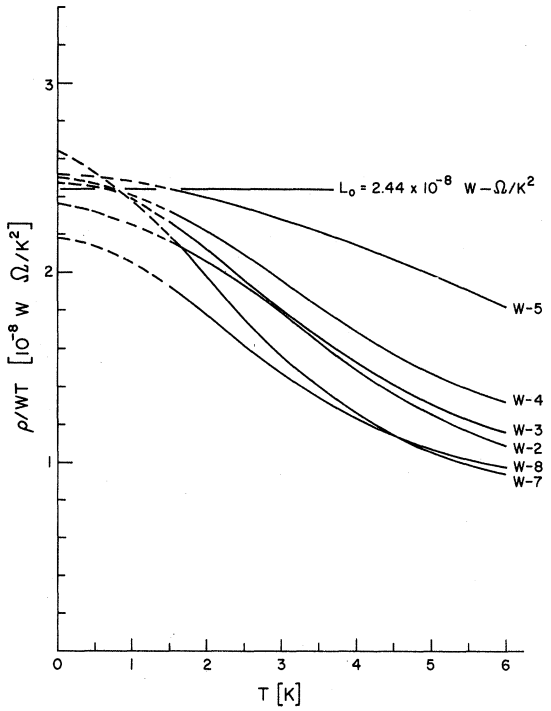

FIG. 6. Variation of the Wiedemann-Franz ratio ρ/WT with temperature for six single-crystal tungsten specimens.

the same as sample W-8. This sample was designated W-8B.

The results of measurements of the resistivities of these two samples are shown in Table I. Most noteworthy are two facts: (i) The Wiedemann-Franz ratio of each sample extrapolates to within a few percent of the Lorenz number as the temperature approaches absolute zero, and (ii) the residual resistance ratio of sample W-8B is 53 000—significantly smaller than the 75 000 residual resistance ratio of sample W-8. A further brief etching of the surface reduced the residual resistance ratio of sample W-8B to only 49 000. These results indicate that the nature of the sample surface may be important in determining the contribution of boundary scattering to the resistivity. It is interesting to conjecture that specular scattering may be responsible for these effects. Although this could explain the sharp decrease in the residual resistance ratio of sample W-8B after the removal of the mirror finish, it is not clear why the Wiedemann-Franz ratio should also be affected. Further experiments as well as a better characterization of the smoothness of the sample surface would help clarify the puzzling behavior of this sample.

From the values of A and α determined from the electrical and thermal resistivity measurements, we have calculated the Lorenz number for electron-electron scattering, $L_e = A/\alpha$, as shown in Table I. This ratio is probably not very meaningful for samples W-8, W-8A, and W-8B because of the size-effect enhancement of A. For the other samples, L_e ranges between 0.2×10^{-8} and 0.4×10^{-8} W Ω/K².

IV. DISCUSSION

A central problem in this investigation has been the separation and identification of the scattering processes important in tungsten at low temperatures. In order to identify each scattering mechanism from the temperature dependence of the resistivity, we felt that it was necessary to perform measurements on enough samples to be able to assess the validity of Matthiessen's rule. The residual resistance ratios of the tungsten samples that we used covered a tenfold range from 9400 to 95 000. Our results indicate that the magnitude of the T^2 term in ρ is not substantially affected by the presence of impurity scattering. On the other hand, with the exception of sample W-8 for which boundary scattering is appreciable, the magnitude of the T^2 term in WT appears to increase systematically with increasing impurity content. These observations are in qualitative agreement with the theoretical calculation of Bennett and Rice.[16]

We have also tried to assess the effect of boundary scattering on the temperature dependence of the resistivities. The temperature dependence of the electrical resistivity is not appreciably affected by the presence of boundary scattering in those samples for which $r_R/d \lesssim 30\,000$ mm^{-1}. However, for greater values of r_R/d, the temperature dependence is enhanced. If a similar effect occurs for WT, it is clear that it is comparable to, or smaller than, the deviations from Matthiessen's rule that we ascribe to impurity scattering.

Our data, and also that of Volkenshteyn[20] and Berthel,[21] show an apparent T^5 behavior of ρ in high-purity samples which is presumably a consequence of electron-phonon scattering. However, we have found no indication of a corresponding T^3 term in WT. At low temperatures, electron-phonon scattering is confined to small angles and is inelastic, so that the Wiedemann-Franz ratio for this type of scattering should be substantially smaller than L_0, i.e., $BT^5/\beta T^3 \ll L_0$, or equivalently $\beta \gg BT^2/L_0$. Using our measured values of B, we estimate that at 6 K, $\beta \gg 2\times10^{-6}$ cm/WK. Although a value as small as 5×10^{-6} cm/WK should be observable, we have been unable to detect any T^3 variation in WT at all.

The principal evidence for the presence of electron-electron scattering in the transition metals is the dominant T^2 dependence of both ρ and WT at low temperatures.[33] To the extent that it is possible to isolate the contribution of electron-

electron scattering to the total resistivities, we have measured the Lorenz number for electron-electron scattering in tungsten and have obtained values ranging from 0.2×10^{-8} to 0.4×10^{-8} W Ω/K^2 for samples W-3, W-4, W-5, W-6, and W-7. These values are significantly below the values calculated by Herring, yet are consistent with the calculation of Bennett and Rice,[16] which does allow lower values of L_e. However, it is doubtful that quantitative agreement with these theories should be expected in tungsten in view of the obvious shortcomings of the two-band model for this metal. Considerable s-d hybridization of the electron wave functions occurs in tungsten, making the distinction between s and d portions of the Fermi surface much less meaningful in tungsten than, for example, in palladium. It may be significant, however, that the theories do allow a decrease in L_e below the Herring values in accord with all the experimental results obtained to date.

ACKNOWLEDGMENTS

The authors are indebted to B. Addis for zone refining the tungsten used in this investigation and to C. Herring whose correspondence prompted this study. We also wish to thank D. Baer for assistance with the experiments and J. W. Wilkins and B. W. Maxfield for helpful discussions.

APPENDIX: COMPUTATION OF THERMAL RESISTIVITY FROM EXPERIMENTAL DATA

The quantities measured in the experiment are $R_1(T)$, $\Delta R(T, \Delta T)$, $\Delta R(T, 0)$, and $\dot{Q}$. By expanding $R_2(T+\Delta T)$ in a Taylor series in ΔT about T, it follows that

$$\Delta R(T, \Delta T) - \Delta R(T, 0) = -R_2'(\Delta T) - \tfrac{1}{2}R_2''(\Delta T)^2 + \cdots , \quad \text{(A1)}$$

where $R_2' = dR_2/dT$ and $R_2'' = d^2R_2/dT^2$. The quadratic term in Eq. (A1) is typically less than 1% of the linear term for temperature differences less than 30 mK. Thus, to first order, the quadratic term can be ignored. In this approximation ΔT is given by

$$\Delta T = -[\Delta R(T, \Delta T) - \Delta R(T, 0)]/R_2' . \quad \text{(A2)}$$

The derivative R_2' is calculated from an analytical fit of the resistance data. We have found it convenient to fit the data to the formula of Clement and Quinell[34]:

$$1/T = a_{-1}/\ln R_2 + a_0 + a_1 \ln R_2 . \quad \text{(A3)}$$

The data are divided into two temperature ranges: 1.5–4.0 K and 3.5–6.5 K. The data in each range are fit by using the two points at each end of the range and one point in the center of the range to determine the three coefficients a_{-1}, a_0, and a_1. The fits obtained in this manner compare favorably with those obtained by a least-squares method. The systematic deviations of the data from the fit are always less than 5 mK. The first derivative R_2' is obtained by differentiating Eq. (A3) with respect to temperature. One obtains

$$R_2' = R_2 \frac{1}{T^2} \frac{\ln R_2}{(a_{-1}/\ln R_2) - a_1 \ln R_2} . \quad \text{(A4)}$$

In practice, Eq. (A3) is used to calculate T from the measured value of $R_2(T) = R_1(T) - \Delta R(T, 0)$. Then Eqs. (A2) and (A4) are used to calculate ΔT.

There are two sources of systematic error in this method: The first arises from the neglect of the small quadratic term in Eq. (A1), and the second from the fact that the actual temperature and the temperature that one calculates by Eq. (A3) differ by a small amount $\epsilon(T)$ because of the difficulty of fitting the data within the experimental error.

In the first case, the effect of the quadratic term is to multiply ΔT by the factor $[1 - \frac{1}{2}(R_2''/R_2')(\Delta T)]$. The second derivative R_2'' can be calculated from Eq. (A4). One obtains

$$\frac{R_2''}{R_2'} = -\frac{2}{T} + \frac{R_2'}{R_2}\left(1 + \frac{2a_{-1}T^2}{(\ln R_2)^3}\frac{R_2'}{R_2}\right) . \quad \text{(A5)}$$

In the second case, the effect of $\epsilon(T)$ on WT can be calculated by replacing T in Eq. (A3) by $T - \epsilon(T)$. One finds that to first order in ϵ the actual value of WT is obtained by multiplying the calculated value of WT by $[1 - (\epsilon/T) + (d\epsilon/dT)]$. Typically, we find that $|d\epsilon/dT| \lesssim 0.02$ and $|\epsilon/T| \lesssim 0.002$. The quantity ϵ and its derivative can be determined with a precision of about 40%. Consequently, after making these corrections, we are able to reduce the total systematic error in the thermal resistivity to a value of less than 1%.

†Work supported by the Atomic Energy Commission under Contract No. AT(30-1)-2150, Technical Report No. NYO-2150-67, and by the Advanced Research Projects Agency through the Materials Science Center at Cornell University, MSC Report No. 1501.

[1]G. K. White and R. J. Tainsh, Phys. Rev. Letters 19, 165 (1967).
[2]J. T. Schriempf, J. Phys. Chem. Solids 28, 2581 (1967).
[3]J. T. Schriempf, Phys. Rev. Letters 19, 1131 (1967).
[4]J. T. Schriempf, Phys. Rev. Letters 20, 1034 (1968).
[5]J. T. Schriempf, Solid State Commun. 6, 873 (1968).
[6]A. C. Anderson, R. E. Peterson, and J. E. Robichaux, Phys. Rev. Letters 20, 459 (1968).
[7]J. G. Beitchman, C. W. Trussel, and R. V. Coleman, Phys. Rev. Letters 25, 1291 (1970).
[8]See, for example, W. J. de Haas and J. de Boer, Physica 1, 609 (1933); G. K. White and S. B. Woods,

Phil. Trans. Roy. Soc. London A251, 273 (1959).
[9]W. G. Baber, Proc. Roy. Soc. (London) A158, 383 (1937); for a general discussion of electron-electron scattering, see N. F. Mott, Advan. Phys. 13, 405 (1964).
[10]There has been some controversy over the interpretation of the results of Ref. 1; see F. C. Schwerer and J. Silcox, Phys. Rev. Letters 20, 101 (1968); and A. Fert and I. A. Campbell, *ibid.* 21, 1190 (1968).
[11]In Os the T^2 term in WT was obscured by electron-phonon scattering which contributes a T^3 term to WT.
[12]C. Herring, Phys. Rev. Letters 19, 167 (1967); 19, 684(E) (1967).
[13]C. Herring (private communication).
[14]H. Smith and J. W. Wilkins, Phys. Rev. 183, 624 (1969).
[15]Umklapp processes are not explicitly considered; in their absence the contribution of normal electron-electron scattering to the electrical resistivity vanishes for a spherical Fermi surface.
[16]A. J. Bennett and M. J. Rice, Phys. Rev. 185, 968 (1969).
[17]M. J. Rice, Phys. Rev. Letters 20, 1439 (1968).
[18]J. T. Schriempf, A. I. Schindler, and D. L. Mills, Phys. Rev. 187, 959 (1969). Although this paper deals with *Pd*: Ni alloys in the context of electron-paramagon scattering, a brief discussion of electron-electron scattering in Pd and Re is given on pp. 971 and 972.
[19]J. de Nobel, Physica 23, 349 (1957).
[20]N. V. Volkenshteyn, L. S. Starostina, V. Ye. Startsev, and Ye. P. Romanov, Fiz. Metal. i Metalloved. 18, 888 (1964) [Phys. Metals Metallog. (USSR) 18, 85 (1964)].
[21]K. H. Berthel, Phys. Status Solidi 5, 399 (1964).
[22]By low temperatures, it is meant temperatures for which $\rho_0 > \frac{1}{2}(\rho - \rho_0)$. The coefficient of T^2 quoted in the translation of Ref. 19 is in error; the value quoted in the original article is smaller by a factor of 10.
[23]G. J. van den Berg, Physica 14, 111 (1948).
[24]G. K. White and S. B. Woods, Can. J. Phys. 35, 656 (1957).
[25]K. H. Berthel, Phys. Status Solidi 5, 159 (1964).
[26]V. Ye. Startsev, N. V. Volkenshteyn, and G. Q. Nikitina, Fiz. Metal. i Metalloved. 26, 261 (1968) [Phys. Metals Metallog. (USSR) 26, 76 (1968)].
[27]56 Ω, $\frac{1}{10}$ W, Allen Bradley Co., Milwaukee, Wisc. The resistors used were matched to about 1% at 4.2 K.
[28]CR2500L, Cryocal Inc., Riviera Beach, Fla.
[29]J. W. Ekin and D. K. Wagner, Rev. Sci. Instr. 41, 1109 (1970).
[30]Molecular sieve, Union Carbide International Co., New York, N. Y.
[31]See for example, *The Physics of Metals I. Electrons*, edited by J. M. Ziman (Cambridge U. P., Cambridge, England, 1969), pp. 185–9.
[32]G. V. Chester and A. Thellung, Proc. Roy. Soc. (London) 77, 1005 (1961).
[33]New independent evidence for electron-electron scattering has been obtained in field-emission studies of tungsten at 20 K; C. Lea and R. Gomer, Phys. Rev. Letters 25, 804 (1970).
[34]J. R. Clement and E. H. Quinell, Rev. Sci. Instr. 23, 213 (1952).

PHYSICAL REVIEW B VOLUME 3, NUMBER 10 15 MAY 1971

Anisotropic Electron-Phonon Coupling*

F. David Peat
Division of Chemistry, National Research Council of Canada, Ottawa, Canada
(Received 15 October 1970)

The interaction between electrons and "pseudolongitudinal" or "pseudotransverse" phonons is derived and used in the calculation of renormalized phonon modes. Coupled modes involving plasmon and optical pseudolongitudinal or pseudotransverse phonons are expected to give rise to observable anisotropic results in Raman scattering.

I. INTRODUCTION

Wave motion in homogenous isotropic media is capable of a convenient representation in terms of transverse and longitudinal modes. In the case of real elastic media, such a decomposition becomes idealized, sound waves moving near to a surface or light passing through an anisotropic medium may not be discussed in terms of purely irrotational or divergence free waves. Similarly the lattice vibrations of many crystals are not purely longitudinal or transverse except in certain particular directions. The treatment of phonons and of electron-phonon interaction in solid-state physics is usually based upon an isotropic model for the crystal. If such a model is augmented in favor of one displaying some on the anisotropies of real crystals it becomes interesting to consider the consequences. In Sec. II of this paper an anisotropic electron-phonon interaction is derived and used in Sec. III to determine the renormalization of the acoustic modes and of the electron gas. Some of the consequences are outlined in Sec. IV together with a discussion of the possibility of the existence of observable effects. Finally in Sec. V the mixed optical phonon and phonon modes are derived and their significance in Raman scattering discussed.

II. ANISOTROPIC ELECTRON-PHONON COUPLING

In a crystal, having a single ion in each cell, the